Hyperspectral at-sensor radiance for aerosol and surface reflectance retrievals

Cristiana Bassani[1], **Rosa Maria Cavalli**[1], **Sergio Ugo de Ceglie**[2], **Maria Lo Moro**[2]

[1] Institute for Atmospheric Pollution Research (IIA), Italian National Research Council (CNR), Via Fosso del Cavaliere 100, 00133 Rome, Italy

[2] CISAM, Via della bigattiera lato Monte 10, 56010 San Piero a Grado, Pisa, Italy)

cristiana.bassani@lara.rm.cnr.it

Abstract

The retrieval process of aerosol properties and surface reflectance from space data based on simulation of the outgoing reflected and scattered radiation in the Earth-Atmosphere system, are widely used [4, 8, 6, 5]. Concerning hyperspectral data, minimization algorithms solve the inverse problem retrieving the aerosol optical thickness [3, 2, 1] for a given aerosol model. The a priori assumption of the aerosol model could provide inaccurate simulation of the atmospheric radiative field which also relies on phase function of the aerosol. Furthermore, the physically-based atmospheric correction of the hyperspectral remote sensing data provides the surface reflectance starting from the at-sensor radiance [3, 2, 7, 1]. The data processing requirements are the knowledge of the atmospheric state during the data acquisition. The forward problem solution could be unrealistic surface reflectance if the atmospheric parameters are not available and a priori assumed.

1. Methods

THE synthetic spaceborne and airborne hyperspectral radiance, generated for contiguous channels sampled at $2.5nm$ within the spectral domain $400 - 2500nm$, are performed with respect to the aerosol properties, namely the urban and continental model and the optical thickness at 550 nm (AOT). The signal is simulated for at-nadir viewing angle over three surface: sand, vegetation and clear-water. The approach is based on the equation presented in [8] assuming negligible the anisotropy of the surface reflectance (lambertian surface):

$$L(\lambda) = \frac{\mu_s E_s(\lambda)}{\pi} t^g(\lambda)[\rho^{atm}(\lambda) + \frac{T^{\uparrow}(\lambda)T^{\downarrow}(\lambda)\rho_{gnd}(\lambda)}{1 - S(\lambda)\rho_{gnd}(\lambda)} \quad (1)$$

$L(\lambda)$ is the at-sensor radiance; $\mu_s = cos(\theta_s)$ where θ_s is the solar zenith angle; $E_s(\lambda)$ is the solar irradiance at the Top Of Atmosphere (TOA); $t^g(\lambda)$ is the transmittance due to the gas absorption; $\rho^{atm}(\lambda)$ is the intrinsic atmospheric reflectance; $T^{\uparrow}(\lambda)$ and $T^{\downarrow}(\lambda)$ are the total upwelling and downwelling transmittance, both with direct and diffuse components; $S(\lambda)$ is the atmospheric spherical albedo and $\rho_{gnd}(\lambda)$ is the at-ground reflectance. For this study, $\rho_{gnd}(\lambda)$ are sand, vegetation and clear-water (Figure 1).

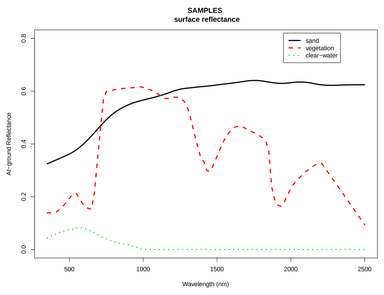

Figure 1: *At-ground reflectance, $\rho_{gnd}(\lambda)$: sand, vegetation and clear-water.*

The straightforward application of the Equation 1 uses the last generation [6] of the Second Simulation of a Satellite Signal in the Solar Spectrum (6S) radiative transfer code [8]. The 6S is an open-source code with a reasonable computational time and with a significant accuracy improvement of the remote sensing results [7].

2. Results

THE hyperspectral data, obtained from the Equation 1, represent the spectral behavior of the at-sensor radiance along the entire spectral domain under different atmospheric conditions defined by:

Aerosol Model $\Rightarrow$ Continental & Urban

Aerosol Optical Thickness $\Rightarrow AOT = \{0.05, 0.30, 0.55, 0.80, 1.05\}$

The simulations are performed for at-nadir viewing three surface reflectance: sand, vegetation and clear-water. Regards the airborne sensor, the aircraft altitude is chosen $1.5km$.

2.1 Continental Model

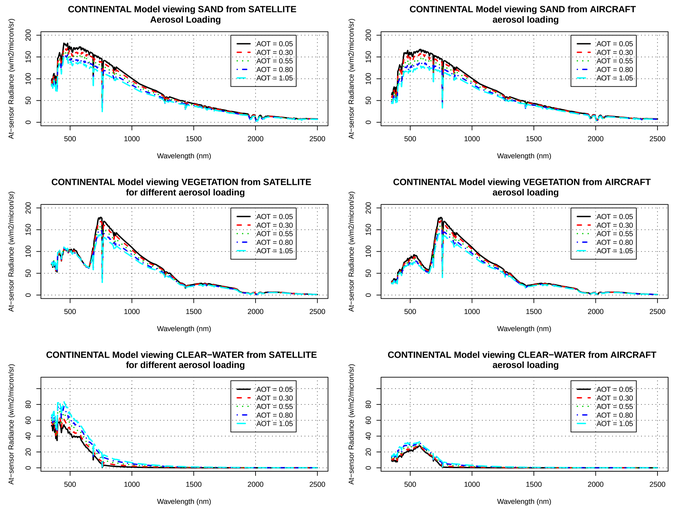

Figure 2: *Nadir at-sensor radiance for airborne and satellite sensor with CONTINENTAL aerosol model for different values of aerosol optical thickness (AOT).*

The Figure 2 shows the spectral at-sensor radiance with continental model. The radiance decreases for high aerosol loading if the surface is bright (sand), on the contrary the radiance increases if the reflectance is low (clear-water). Furthermore, the radiance of the clear-water viewed from satellite is higher than the one observed by aicraft.

2.2 Urban Model

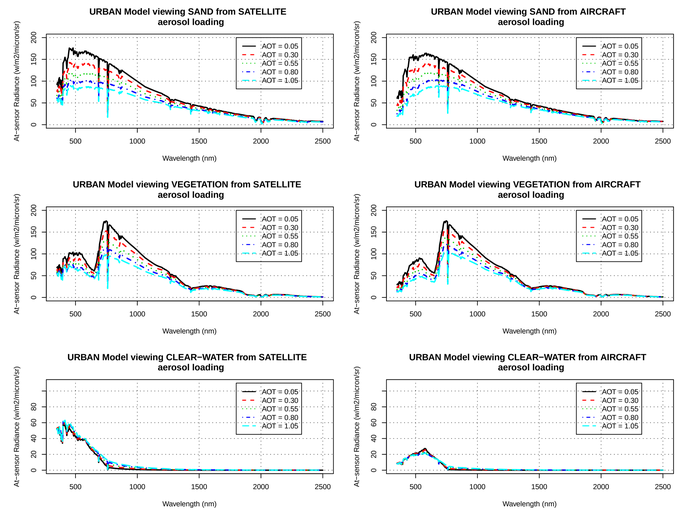

Figure 3: *Nadir at-sensor radiance for airborne and satellite sensor with URBAN aerosol model for different values of aerosol optical thickness (AOT).*

The Figure 3 shows the spectral at-sensor radiance with urban model. The radiance decreases for high aerosol loading if the surface is bright (sand) more than in the case of continental aerosol model. Regards the low reflectance (clear-water), the values of the radiance appear to be independent from the aerosol loading.

3. Conclusion

THE study reveals the potential of hyperspectral data to provide more and better spectral information useful for optical atmospheric study.
The bright surfaces are affected by the aerosol loading principally in case of urban model. Whereas, the aerosol loading has a large impact on the at-sensor radiance for dark surface in case of continental model and cloud be neglected in case of urban model.

References

[1] C. Bassani, R. M. Cavalli, and S. Pignatti, *Aerosol optical retrieval and surface reflectance from airborne remote sensing data over land.*, Sensors, 10 (2010), pp. 6421–6438.

[2] B.-C. Gao, M. J. Montes, C. O. Davis, and A. F. H. Goetz, *Atmospheric correction algorithms for hyperspectral remote sensing data of land and ocean.*, Remote Sensing of Environment, 113 (2009), pp. S17–S24.

[3] L. Guanter, V. Estellés, and J. Moreno, *Spectral calibration and atmospheric correction of ultra-fine spectral and spatial resolution remote sensing data. application to casi-1500 data.*, Remote Sensing of Environment, 109 (2007), pp. 54–65.

[4] Y. J. Kaufman, D. Tanré, H. R. Gordon, T. Nakajima, J. Lenoble, R. Frouin, H. Grassl, B. M. Herman, M. King, and P. M. T. P.M., *Operational remote sensing of tropospheric aerosol over land from eos moderate resolution imaging spectroradiometer*, Journal of Geophysical Research, 102 (1997), pp. 17051–17067.

[5] A. A. Kokhanovsky, J. L. Deuz, D. J. Diner, O. Dubovik, F. Ducos, C. Emde, M. J. Garay, R. G. Grainger, A. Heckel, M. Herman, I. L. Katsev, J. Keller, R. Levy, P. R. J. North, A. S. Prikhach, V. V. Rozanov, A. M. Sayer, Y. Ota, D. Tanr, G. E. Thomas, and E. P. Zege, *The inter-comparison of major satellite aerosol retrieval algorithms using simulated intensity and polarization characteristics of reflected light*, Atmospheric Measurement Techniques, 3 (2010), p. 909932.

[6] S. Y. Kotchenova, E. F. Vermote, R. Levy, and A. Lyapustin, *Radiative transfer codes for atmospheric correction and aerosol retrieval: Intercomparison study*, Applied Optics, 47 (2008), pp. 2215–2226.

[7] E. F. Vermote and S. Kotchenova, *Atmospheric correction for the monitoring of land surfaces.*, Journal of Geophysical Research, 113 (2009), pp. 675–686.

[8] E. F. Vermote, D. Tanré, J. L. Deuzé, M. Herman, and J. J. Morcrette, *Second simulation of the satellite signal in the solar spectrum, 6s: An overview*, IEEE Transactions on Geoscience and Remote Sensing, 35 (1997), pp. 675–686.

EGU 2011, European Geosciences Union General Assembly 2011, 03-08 April 2011, Vienna, Austria